Article

Effects of pH and Dissolved Silicate on Phosphate Mineral-Water Partitioning with Goethite

Md Abdus Sabur,* Christopher T. Parsons, Taylor Maavara, and Philippe Van Cappellen

Cite This: *ACS Earth Space Chem.* 2022, 6, 34–43

Read Online

ACCESS | Metrics & More | Article Recommendations | Supporting Information

ABSTRACT: Release of sorbed phosphate from ferric iron oxyhydroxides can contribute to excessive algal growth in surface water bodies. Dissolved silicate has been hypothesized to facilitate phosphate desorption by competing for mineral surface sites. Here, we conducted phosphate and silicate adsorption experiments with goethite under a wide pH range (3–11), both individually (P or Si) and simultaneously (P plus Si). The entire experimental data set was successfully reproduced by the charge distribution multisite surface complexation (CD-MUSIC) model. Phosphate adsorption was highest under acidic conditions and gradually decreased from near-neutral to alkaline pH conditions. Maximum silicate adsorption, in contrast, occurred under alkaline conditions, peaking around pH 10. The competitive effect of silicate on phosphate adsorption was negligible under acidic conditions, becoming more pronounced under alkaline conditions and elevated molar Si:P ratios (>4). In a subsequent experiment, desorption of phosphate with increasing pH was monitored, in the presence or absence of dissolved silicate. While, as expected, desorption of phosphate was observed during the transition from acidic to alkaline conditions, a fraction of phosphate remained irreversibly bound to goethite. Even at high Si:P ratios and alkaline pH, dissolved silicate did not affect phosphate desorption, implying that kinetic factors prevented silicate from displacing phosphate from goethite binding sites.

KEYWORDS: *competitive adsorption, phosphate, silicate, goethite, CD-MUSIC model*
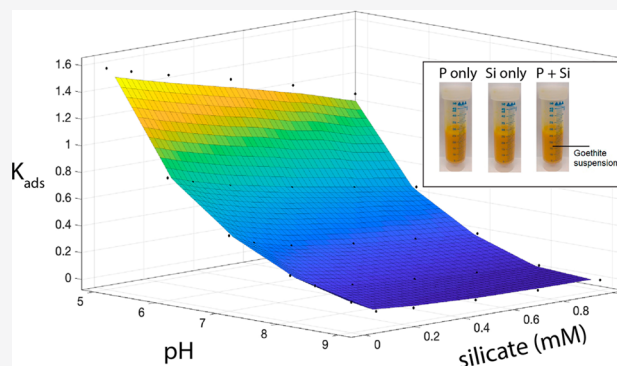
1. INTRODUCTION

Phosphorus (P), in the form of aqueous phosphate, is an essential nutrient for the growth of plants and algae.[1] Because it often limits or colimits primary production in freshwater and nearshore marine systems, phosphate enrichment can result in eutrophication and algal blooms.[2] Dissolved phosphate is supplied to surface waters from external sources, such as runoff from agricultural land and wastewater treatment plant effluent,[3–5] as well as through P recycling from bottom sediments to the water column.[6–12] The latter is also known as internal P loading.

Important removal pathways of aqueous phosphate from surface waters include sorption to minerals and uptake into organic matter,[6,13–16] followed by deposition and incorporation of the particulate phases in sediments. Early diagenetic remobilization of aqueous phosphate can occur as a result of mineral dissolution, desorption, and hydrolysis of particulate organic P.[6,17,18] In particular, the reductive dissolution of phosphate-containing ferric iron (hydr)oxides and the desorption of phosphate from mineral surfaces are generally considered major processes driving internal P loading in lakes. Adsorption and desorption of phosphate can further be modulated by other anionic species, including arsenate,

bicarbonate, sulfate, and silicate, that compete with phosphate for mineral binding sites.[17,19,20]

Among phosphate's anionic competitors, dissolved silicate is ubiquitous in aquatic environments. It occurs predominately in the form of silicic acid (H_4SiO_4) produced by the dissolution of detrital silicate minerals and various forms of biogenic silica.[21,22] According to the data from the US National Water Information System database,[23] the average concentrations of dissolved silicate in groundwater, rivers, and freshwater lakes are around one to a few hundreds of micromolar. In some cases, the concentrations may reach values of 1–2 mM, usually indicating a solubility control by amorphous silica.[24]
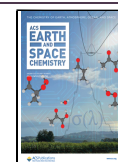
A number of experimental studies have addressed the effect of dissolved silicate on the release of phosphate from natural aquatic sediments[25–28] as well as from agricultural soils.[29] Natural sediments, however, are inherently complex with many

constituents and processes potentially contributing to aqueous phosphate mobilization. For example, hydrolysis of particulate organic-P may lead to an overestimation of phosphate release from mineral phases if the latter is the only mechanism considered.[30] Similarly, the dissolution of diatom frustules can release both silicate[27] and phosphate[31] to solution, thus potentially confounding the interpretation of the effect of silicate on phosphate release from sediments. Alternatively, pure end-member sorbent materials can be used to probe specific processes controlling aqueous phosphate removal or release.

Previous studies have focused on the adsorption of phosphate[20,32,33] and silicate[34−36] on ferric iron (hydr)oxides, but separately from one another. Therefore, the effects of dissolved silicate on phosphate immobilization by, and release from, Fe(III) (hydr)oxides surfaces still require further investigation. In a recent study, Hiemstra[37] did show that aqueous silicate decreases phosphate adsorption to ferrihydrite under alkaline pH conditions. That study, however, did not consider the role of the aqueous Si:P ratio in modulating the competition for binding sites. In addition, the influence of dissolved silicate on phosphate desorption from ferric iron (hydr)oxides has yet to be addressed.

In this study, a series of batch adsorption experiments were conducted to derive the equilibrium adsorption envelopes of phosphate and silicate as a function of pH, both individually (P or Si) and simultaneously (P plus Si). Goethite was chosen as the sorbent because it is a stable and ubiquitous iron mineral with a relatively large surface area ($10−132$ m^2/g).[38] The combined experimental results were used to optimize parameter values for the triple layer charge distribution multisite surface complexation (CD-MUSIC) model. This model has been previously used in separate studies on the adsorption of aqueous phosphate and silicate onto goethite.[34,39] The optimized model was then used to explore the adsorption of phosphate and silicate over broad ranges of aqueous Si:P ratios, pH, and background electrolyte concentration, as well as to assess the reversibility of phosphate desorption with or without dissolved silicate present.

2. MATERIALS AND METHODS

2.1. Chemicals. Goethite (Bayferrox 910 MU) was purified through 12 repetitive washes with 18.2 MΩ cm^{-1} water followed by centrifugation, ensuring that the conductivity of the supernatant no longer changed. The specific surface area of 15.0 m^2/g was determined by the nitrogen gas adsorption method using a Gemini VII instrument. The point of zero net proton charge (PZC) of 10.0 was measured by potentiometric titration following Vakros et al.[40]

Solutions of phosphate and silicate were prepared by dissolving sodium phosphate monobasic (Sigma-Aldrich, H_2NaPO_4, ≥99.0%) and sodium metasilicate nanohydrate (Aldrich, $Na_2SiO_3 \cdot 9H_2O$, ≥98.0%), respectively, in background solutions of 10 mM NaCl (Fisher Scientific, 99.0%) and 1 mM N-(2-hydroxyethyl)piperazine-N′-2-ethanesulfonic acid (HEPES) (Fisher Scientific, $C_8H_{18}N_2O_4S$, ≥99%). HEPES was selected to minimize pH drift during the adsorption experiments. As shown previously, HEPES has no measurable competitive effect on the adsorption of anions, including phosphate, on ferric iron (hydr)oxides.[41] Unless otherwise stated all solutions and reagents were prepared using 18.2 MΩ cm^{-1} water (Millipore). The pH of the solutions was adjusted using NaOH and HCl. The exact amount of goethite used in

each experiment was determined by weighing the adsorption vial on an analytical balance with a precision of 0.01 mg. All experiments were performed at least twice to verify reproducibility. An anaerobic chamber (Coy laboratory products) with a <1 ppmv O_2, 97% N_2, 3% H_2 atmosphere was used for all experiments to avoid interference from bicarbonate derived from atmospheric CO_2.

2.2. Analytical Methods. To avoid the interference from dissolved silicate in the colorimetric determination of dissolved phosphate,[42] inductively coupled plasma optical emission spectroscopy (ICP-OES, Thermo Scientific iCAP 6300) was used to measure total aqueous concentrations of iron, phosphate, and silicate (as elemental Fe, P, and Si) after acidification with ultrapure HNO_3 (EMD Millipore Corporation) to <pH 2. Precision was <5% RSD and accuracy ±10% with respect to NIST validated solutions for all analytes. Three wavelengths per analyte were selected and evaluated to ensure minimal interference from other solution components. The method detection limits for Fe, P, and Si were 0.89, 1.61, 1.78 μM, respectively. Matrix-matched standards were used for calibrations and all reagents were prepared with analytical grade salts from isoSPEC and 18.2 MΩ cm^{-1} water (Millipore).

2.3. Experiments. *2.3.1. Adsorption Experiments.* Separate solutions of 50 μM phosphate and silicate, as well as a combined solution of phosphate and silicate (50 μM each), were prepared in 10 mM NaCl background electrolyte solution containing 1.0 mM HEPES. The pH of the solutions was adjusted between pH 2 and 12 using 0.1 and 1.0 M NaOH and HCl, respectively. The solutions (25 mL) were added to polypropylene centrifuge tubes (VWR, 50 mL) each containing 0.0125 g of goethite (0.5 g/L). The suspensions were agitated on a rotary shaker at 30 rpm (Glass-Col, 099A RD4512) at 25 °C for 6 h to allow equilibration of the goethite with phosphate and silicate, individually and in combination. The 6 h equilibration time was determined in preliminary adsorption kinetics experiments for phosphate and silicate (see Supporting Information Figure S1). Although HEPES only acts as a buffer between pH 6.8 and 8.2, it was added in all the suspensions for consistency. After pH adjustments, aliquots of each solution were taken before mixing with goethite to determine initial elemental concentrations by ICP-OES. At the end of an experiment the centrifuge tubes were centrifuged at 1690 RCF for 15 min (Thermo Scientific, Sorvall ST 16R). The supernatant was filtered through 0.45 μm pore size polypropylene (VWR Scientific Inc.) syringe filters and the pH of the filtrate was immediately remeasured. Filtrates were acidified to less than pH 2 with ultrapure nitric acid and stored at 4 °C until analysis by ICP-OES.

2.3.2. Surface Complexation Modeling. Here, we use the charge distribution multisite surface complexation (CD-MUSIC) model, a triple layer model based on the valence bond theory that, in turn, builds on Pauling's valence bond concept. The valence bond theory has been used to interpret crystal structures. The CD-MUSIC, initially developed by Hiemstra et al.[43,44] and Hiemstra and van Riemsdijk,[45] extends the theory to crystal surfaces to describe the chemical structure of metal (hydr)oxide-aqueous solution interfaces. Most importantly, the CD-MUSIC model is able to account for the adsorption of multiple competing anions, including phosphate and arsenate, phosphate and selenite, plus phosphate and carbonate.[33,46] The CD-MUSIC model is

Table 1. Surface Complexation Reactions and Respective CD-MUSIC Model Parameters for the Adsorption of Phosphate and Silicate on Goethite at 25 °C[a]

reaction	log K	Δz_0	Δz_1
Goethite (3.45 sites/nm^2 (singly coordinated groups), 2.7 sites/nm^2 (triply coordinated groups), $C_1 = C_2 = 0.92$ F/m^2);[34] the surface reactions 1–2 including their Δz_0 and Δz_1 are taken from the work of Kinniburgh and Copper[53] and the log K values are set to 10 as inferred from the measured PZC of goethite (see section 2.1)			
(1) $\equiv Fe_3O^{-0.5} + H^+ \rightleftharpoons \equiv Fe_3OH^{+0.5}$	10.0	1	0
(2) $\equiv FeFeOH^{-0.5} + H^+ \rightleftharpoons \equiv FeOH_2^{+0.5}$	10.0	1	0
(3) $\equiv FeOH^{-0.5} + Na^+ \rightleftharpoons \equiv FeOHNa^{+0.5}$	-0.6^b	0^b	1^b
(4) $\equiv FeOH^{-0.5} + H^+ + Cl^- \rightleftharpoons \equiv FeOH_2Cl^{-0.5}$	9.5	1^b	-1^b
(5) $\equiv Fe_3O^{-0.5} + Na^+ \rightleftharpoons \equiv Fe_3ONa^{+0.5}$	-0.6^b	0^b	1^b
(6) $\equiv Fe_3O^{-0.5} + H^+ + Cl^- \rightleftharpoons \equiv Fe_3OHCl^{-0.5}$	9.5	1^b	-1^b
(7) $\equiv FeOH^{-0.5} + 2H^+ + PO_4^{-3} \rightleftharpoons \equiv FeOPO_2OH^{-1.5} + H_2O$	27.25 (27.97,[c] 27.65,[d] 19.64,[e] 26.36[f])	0.32 (0.40,[c] 0.28,[d,f] 0.22[e])	-1.32 (-1.40,[c] -1.28,[d,f] -2.22[e])
(8) $2\equiv FeOH^{-0.5} + 2H^+ + PO_4^{-3} \rightleftharpoons (\equiv FeO)_2PO_2^{-2} + 2H_2O$	28.45 (29.69,[c] 29.77,[d] 27.73,[e] 28.31[f])	0.46[d,e,f] (0.48[c])	-1.46[d,e,f] (-1.48[c])
(9) $2\equiv FeOH^{-0.5} + 2H^+ + PO_4^{-3} + H^+ \rightleftharpoons (\equiv FeO)_2POOH^- + 2H_2O$	33.52[f] (34.4,[c] 32.06[e])	0.65[f] (0.82,[c] 0.58,[d] 0.63[e])	-0.65[f] (-0.82,[c] 0.58,[d] -0.63[e])
(10) $2\equiv FeOH^{-0.5} + H_4SiO_4 \rightleftharpoons (\equiv FeO)_2Si(OH)_2^{-1} + 2H_2O$	5.75 (5.85[g])	0.40 (0.29[g])	-0.30 (-0.29[g])
(11) $2\equiv FeOH^{-0.5} + 4H_4SiO_4 \rightleftharpoons (\equiv FeO)_2SiOHOSi_3O_2(OH)_7^{-1} + 5H_2O$	13.98[g]	0.29[g]	-0.29[g]
(12) $2\equiv FeOH^{-0.5} + 4H_4SiO_4 \rightleftharpoons (\equiv FeO)_2SiOHOSi_3O_3(OH)_6^{-2} + 4H_2O + 3H+$	7.47[g] (6.15[h])	0.29[g]	-0.29[g]

[a]The value of log K represents the equilibrium constant for a given surface complexation reaction, and Δz_0 and Δz_1 indicate the change of charge upon formation of a complex at the 0- and 1-plane, respectively. The Δz_2 values in the model were assumed to be 0 (zero) for all the surface species, and, thus, they are not shown here. When multiple parameter values are shown, the value outside the brackets was used in this study. This study: H$_2$NaPO$_4$ (50 μM), Na$_2$SiO$_3$·9H$_2$O (50–1000 μM), goethite (0.5 g/L, 15.0 m^2/g, PZC = 10), NaCl (0.01 M), 6 h at RT, ICP-OES. [b]Rahnemaie et al.:[51] NaCl (0.01–0.1 M), goethite (3.0–10.0 g/L, 85 m^2/g, PZC = 8.5 and 9.0 in LiCl and NaCl solution, respectively), at 20.0 ± 0.1 °C. [c]Rahnemaie et al.:[39] NaHPO$_4$ (0.01–10 mM) in NaNO$_3$ (0.05–0.5 M), goethite (2.5–10 g/L, 100 m^2/g, PZC = 9.2), 24 h at 20 °C, Mo-blue method. [d]Stachowicz et al.:[33] NaNO$_3$ (0.01–0.1 M), phosphate (0.25–0.75 mM), goethite (5 g/L, 100 m^2/g, PZC = 9.2), 24 h at 22 °C, ICP-AES. [e]Antelo et al.:[48] NaNO$_3$ (0.01–0.5 M), 24 h at 25 °C, ferrihydrite (1.0 g/L, 350 m^2/g, PZC = 8.7), Mo-blue method. [f]Hiemstra:[37] NaHPO$_4$ (0.039 mM), Na$_2$SiO$_3$·9H$_2$O (0.1–1.0 mM), NaNO$_3$ (0.01–2.0 M), ferrihydrite (0.12–0.40 g/L, PZC = 8.1, 610 m^2/g), Mo-blue method. [g]Hiemstra et al.:[34] Na$_2$SiO$_3$·9H$_2$O (0.1–1 mM), NaNO$_3$ (0.1 M), 1–3 g/L goethite (100 m^2/g), Mo-blue method. [h]Kersten and Vlasova:[50] Na$_2$SiO$_3$·9H$_2$O (10–100 μM), goethite (1 g/L, 20 m^2/g, PZC = 9.1), NaNO$_3$ (10–100 mM), 24 h at 10–25 °C, Mo-blue method.

therefore well-equipped to account for the simultaneous adsorption of phosphate and silicate.

The CD-MUSIC model considers singly $\equiv FeOH(H)$ and triply $\equiv Fe_3O(H)$ coordinated Fe–O surface groups (where "$\equiv$" represents the mineral surface lattice) as active complexation sites on goethite.[45,47] The doubly coordinated surface $\equiv Fe_2O(H)$ group is assumed to be inert over a wide pH range and unlikely to contribute to the PZC of goethite.[45] For the singly $\equiv FeOH(H)$ and triply $\equiv Fe_3O(H)$ coordinated surface groups, the log K values have been proposed to be very close.[47] For simplicity, we assumed that both surface groups behave similarly in surface protonation/deprotonation reactions and in their interactions with the electrolyte ions. However, only the singly coordinated Fe–O surface groups were considered as possible binding sites when writing the surface complex formation reactions with phosphate and silicate.[47]

In the CD-MUSIC model, the overall capacitance of the metal (hydr)oxide–water interface is the combination of the inner and outer Stern layer capacitances.[47] The types of surface complexes represented in the model are usually inferred from spectroscopic evidence.[34,37,39,48] The complexation reactions then describe the partial neutralization of the surface charge as the oxyanion binds to the surface. For example, the adsorption of aqueous H$_4$SiO$_4$ on a singly coordinated $\equiv FeOH^{-0.5}$ surface group of goethite leads to changes in the electrical charges Δz_0 and Δz_1 in the 0- and 1-planes, respectively, according to the following stoichiometric equation:

$$2\equiv FeOH^{-0.5} + H_4SiO_4^0 \rightleftharpoons \equiv Fe_2O_2^{-1+\Delta z_0}Si(OH)_2^{\Delta z_1} + 2H_2O \tag{1}$$
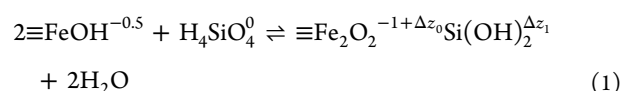
The interfacial charge distribution (CD) values (Δz) are obtained by optimizing the geometry of the surface complexes with the Brown bond valence approach[49] using molecular orbital calculations by density functional theory.[34,37,39,50] The Δz values, however, may vary slightly depending on the experimental conditions, e.g., ionic strength, temperature, background electrolyte composition, nature of the counterions, and sorbent properties.[34,37,39,50] The CD-MUSIC model parameters also depend on the choice of surface reactions used to fit the experimental data.[34,37,39,50]

The surface complexation reactions for phosphate and silicate considered here are those proposed by Rahnemaie et al.[51] and Hiemstra et al.,[34] respectively. Thus, for the phosphate, monoprotonated monodentate $\equiv FeOPO_2OH^{-1.5}$, monoprotonated bidentate $(\equiv FeOO)_2POOH^-$, and unprotonated bidentate $(\equiv FeO)_2PO_2^{-2}$ complexes were included (reactions 7, 8, and 9 in Table 1). For silicate, bidentate monomer $(\equiv FeO)_2Si(OH)_2^{-1}$, tetramer $(\equiv FeO)_2SiOHOSi_3O_2(OH)_7^{-1}$, and polymer surface complexes $(\equiv FeO)_2SiOHOSi_3O_3(OH)_6^{-2}$ (reactions 10, 11, and 12 in Table 1) were included. The previously reported surface site densities and the Stern layer capacitance for goethite (Table 1) plus the specific surface area and the PZC of goethite determined in this study (section 2.1) were imposed in the model. The CD-MUSIC model was implemented in conjunction with PHREEQC Version 3 and the phreeqc.dat

database to account for variations in aqueous phase speciation.[52]

As a starting point for fitting the model to the entire set of experimental data, that is, both individual and simultaneous adsorption of phosphate and silicate data, Δz and $\log K$ values reported previously were used as initial estimates (see Table 1).[34,37,39,47,48] Deviations of these values were expected, however, because of differences in experimental conditions (see footnotes in Table 1). The Δz and $\log K$ values were manually adjusted by trial and error until a global fit to the entire data set was achieved. Goodness-of-fit was estimated using the root-mean-square error (RMSE) (see Supporting Information section SM-2.1). The final parameter values are listed in Table 1. Admittedly, this parameter set is nonunique, and slightly different values may yield an equally good fit to the data.

As mentioned earlier, the modeling calculations are performed using PHREEQC 3 with the pheeqc.dat database.[52] Therefore, in addition to reactions 1 to 12 identified in Table 1, two additional surface reactions are listed in Table 2

Table 2. Additional Surface Complexation Reactions and the Respective CD-MUSIC Model Parameters Used in This Study for the Estimation of Phosphate and Silicate Adsorption with PHREEQC[a]

reaction	$\log K$	Δz_0	Δz_1
(13) $\equiv Fe_3OH_{0.5} \rightleftharpoons \equiv Fe_3O^{-0.5} + 0.5H^+$	10	−0.5	0
(14) $\equiv FeOH_{1.5} \rightleftharpoons \equiv FeOH^{-0.5} + 0.5H^+$	10	−0.5	0

[a]Please see the caption of Table 1 for further information.

(Reactions 13 and 14) because they are built into the PHREEQC codes.[53] While Reactions 13 and 14 have nonsignificant contributions in proton binding, the neutral species $\equiv Fe_3OH_{0.5}$ and $\equiv FeOH_{1.5}$ in the reactions are important for coupling surface sites and when varying the goethite concentration.[53]

2.3.3. Phosphate Desorption Experiment. A suspension was prepared by equilibrating goethite (0.5 g/L) in 1197 mL of 10 mM NaCl solution for 24 h, during which the pH dropped from 6 to 5. Next, 3 mL of 10 mM phosphate solution was injected into the suspension giving a phosphate concentration of 25 μM. The goethite suspension with phosphate was equilibrated for 24 h. Afterward the pH was

lowered to 3 by adding HCl and equilibrated for a further 6 h. Next, an 11 mL aliquot was collected and the pH was increased stepwise by one pH unit increments using NaOH until pH 11 was reached. At each pH an aliquot was collected after 6 h to determine how much adsorbed phosphate was released to solution. The 6 h equilibration time at each pH step was based on preliminary kinetic experiments (see Supporting Information Figure S2).

To investigate the effect of silicate on phosphate desorption, goethite was pre-equilibrated with phosphate at pH 3, as per the previous experiment. An 11 mL aliquot was collected after 6 h of equilibration. Then 4.30 mL of 100 mM silicate was added resulting in a total silicate concentration of 355 μM, i.e., a molar Si:P of 14.2. The addition of silicate caused pH to increase to ∼3.5, which was readjusted to 3 and equilibrated for 6 more hours. The stepwise change of pH from 3 to 11 and the collection of aliquots were performed as in the silicate-free desorption experiment. Each aliquot was centrifuged, filtered, and stored at 4 °C for analysis by ICP-OES as previously described.
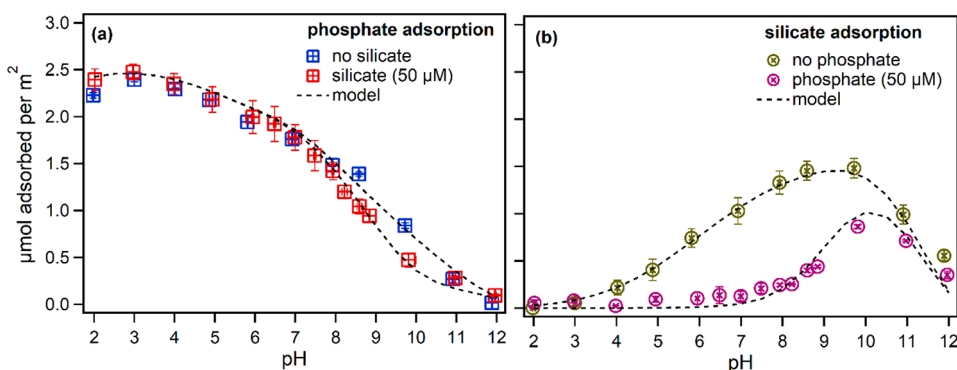
3. RESULTS AND DISCUSSION

3.1. Phosphate and Silicate Adsorption: Data and CD-MUSIC Modeling.
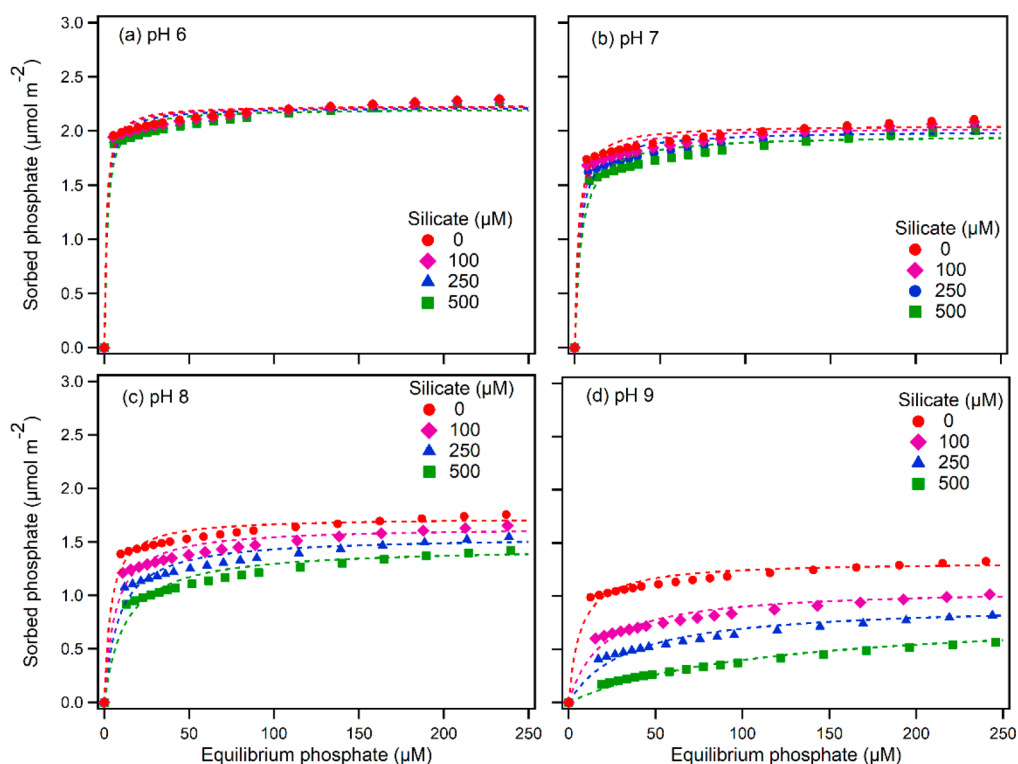Adsorption of phosphate and silicate

Table 3. Calculated RMSE and Chi-Squared (χ^2) Values between the Experimental Data and Model Calculations (Shown in Figure 1) for the Adsorption of Phosphate (50 μM) and Silicate (50 μM) on Goethite (0.5 g/L) at 25 °C and I = 10 mM NaCl[a]

adsorption	sorbate	RMSE	χ^2	χ_c^2
individual	phosphate	0.11	0.16	3.94
	silicate	0.10	0.45	
simultaneous	phosphate	0.06	0.12	6.57
	silicate	0.09	0.69	

[a]The critical chi-squared (χ_c^2) values based on the degrees of freedom are shown beside the observed χ^2 values.

on Fe(III) (hydr)oxides is a function of the pH-dependent surface charge and aqueous speciation of the sorbates. The dominant aqueous species of H_3PO_4 at pH 7 are the deprotonated forms $H_2PO_4^-$ and HPO_4^{2-} (see Supporting Information Figure S3a). Under moderately acidic conditions,

Figure 1. Individual and simultaneous adsorption of phosphate and silicate (50 μM each) on goethite (0.5 g/L) at 25 °C and I = 10 mM NaCl, between pH 2 and 12. Experimental results (markers) and predictions by CD-MUSIC model (dashed lines) are shown for (a) adsorption of phosphate (50 μM) in the absence and presence of silicate (50 μM); (b) adsorption of silicate (50 μM) in the absence and presence of phosphate (50 μM). Error bars represent the range of values measured between duplicate experiments.

Figure 2. Phosphate adsorption (points) calculated by the CD-MUSIC model in the presence of various concentrations of silicate (0, 100, 250, 500 μM) on goethite (0.5 g/L) at 25 °C and I = 10 mM NaCl, as a function of pH. The Langmuir adsorption isotherms (eq 2) fitted to the phosphate adsorption data predicted with the CD-MUSIC model are shown by the dashed lines.

the singly deprotonated $H_2PO_4^-$ dominates although the fully protonated form H_3PO_4 also exists as a minor fraction under extremely acidic conditions (pH $\leq$ 2). Silicic acid in solution exists as neutral H_4SiO_4 up to pH 8 beyond which the deprotonated $H_3SiO_4^-$ increases and becomes dominant above the pK_a of silicic acid (pH 9.84) (see Supporting Information Figure S3b).

Experimental results for the individual and simultaneous adsorption of phosphate and silicate are shown in Figure 1 (also see Figure S4 in the Supporting Information). As observed by previous researchers,[39,54,55] the adsorption of phosphate on goethite is maximal below pH 4 and decreases as the pH in solution increases (Figure 1a). With increasing pH, electrostatic attraction becomes increasingly less favorable as the goethite surface becomes less positively charged,[39,55] despite the transition to increasingly deprotonated phosphate species.

Silicate adsorption to goethite is quite different from that of phosphate, with limited binding below pH 3.[34,56] In the absence of phosphate, silicate adsorption increases with pH and reaches its maximum around the PZC of goethite (pH 10, Figure 1b). Beyond pH 10, silicate adsorption decreases again even as the concentration of the deprotonated $H_3SiO_4^-$ exceeds that of undissociated silicic acid. Because the goethite surface charge is negative above pH 10, electrostatic repulsion between an increasingly negatively charged surface and deprotonated $H_3SiO_4^-$ helps explain the decreased adsorption of silicate.

In the adsorption experiments where both phosphate and silicate are present, the two sorbates can compete for the surface sites on goethite. Silicate at equimolar concentrations with phosphate slightly decreases phosphate adsorption under alkaline conditions (e.g., 4% at pH 8), with no significant effect

below pH 7 (Figure 1a). By contrast, adsorption of silicate is strongly diminished by aqueous phosphate over a wide pH range (Figure 1b). For example, in the pH range 3−7 very little adsorption of silicate is observed when phosphate is present. Furthermore, in the single sorbate experiments, the amount of adsorbed silicate on goethite exceeded that of phosphate above pH 8, while in the dual sorbate experiments, this happens above pH 9 (see Supporting Information Figure S4a). Nevertheless, even when competing with phosphate, adsorption of silicate reached a maximum around pH 10 (Figure 1b). The weak influence of silicate on phosphate adsorption and strong influence of phosphate on silicate adsorption are also evident in the phosphate and silicate adsorption kinetics experiments at pH 7 (see Supporting Information Table S1).

As shown in Figure 1, the CD-MUSIC model accurately reproduces the experimental data (see the low RMSE and chi-squared values in Table 3). Because the nature of surface complexes may change depending on the surface loading,[37,39] the performance of the model was further verified against additional experimental data with simultaneous phosphate and silicate sorption at much higher Si:P ratios and absolute concentrations (see Supporting Information Figure S5).

3.2. Phosphate Adsorption: Langmuir Isotherms. Dissolved silicate concentrations in natural freshwaters are generally much higher than those of dissolved phosphate (see Supporting Information Figure S6). Aqueous Si:P ratios are also highly variable and, as such, conducting laboratory experiments to cover the entire range of all possible dissolved silicate and phosphate concentrations, Si:P ratios, pH, and other solution properties would be extremely onerous. Alternatively, we can use the CD-MUSIC model to explore the competitive effect of silicate on the adsorption of phosphate on goethite under environmental conditions beyond
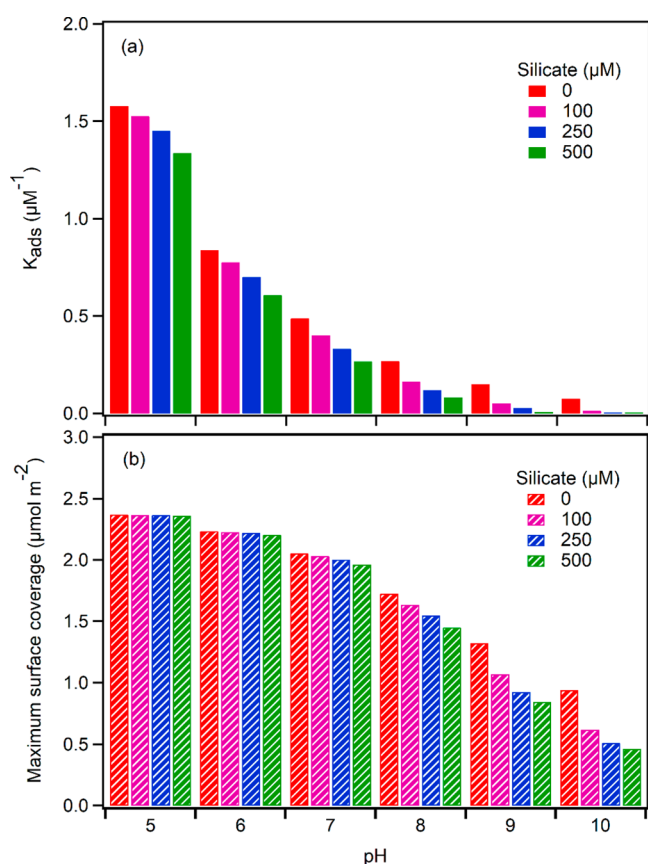
Figure 3. Langmuir constants (K_{ads}) and maximum surface coverage (θ_{max}) for the adsorption of phosphate on goethite (0.5 g/L) in the presence of various silicate concentrations (0, 100, 250, 500 μM) at 25 °C and I = 10 mM NaCl, as a function of pH. The K_{ads} and θ_{max} values are extracted by fitting the CD-MUSIC model predicted phosphate adsorption data (shown in Figure 2) to eq 2.

those investigated in the laboratory. However, while the CD-MUSIC model is an effective tool to predictively understand adsorption phenomena based on a detailed mechanistic representation of the chemical and electrical structure of the mineral−water interface, it may be relatively cumbersome for routine applications.

A commonly used empirical adsorption model is the Langmuir adsorption isotherm.[57] We therefore fitted the following Langmuir isotherm expression to adsorbed phosphate concentrations predicted with the CD-MUSIC model:

$$\theta = \theta_{max}\frac{K_{ads}[A]}{1 + K_{ads}[A]} \tag{2}$$

where θ is the amount of phosphate covering the goethite surface (μmol/m^2) at a given pH and dissolved silicate concentration, $[A]$ is the equilibrium aqueous phosphate concentration (μM), θ_{max} is the maximum surface coverage of phosphate, and K_{ads} (μM^{-1}) denotes the Langmuir adsorption constant. The fitted Langmuir isotherms for environmentally relevant ranges of dissolved phosphate (20−250 μM) and silicate (0−500 μM) concentrations, and pH ranging from 6 to 9, are shown in Figure 2. The corresponding values of K_{ads} and θ_{max} are in Figure 3.

The K_{ads} and θ_{max} values are quite variable: both parameters decrease with increasing pH and increasing aqueous silicate concentration. For example, as the concentration of aqueous

silicate increases from 100 to 500 μM, K_{ads} decreases by 22% at pH 6 and by 83% at pH 9. At the same time, θ_{max} drops by 1% and 21% at pH 6 and 9, respectively. The lower the K_{ads} and θ_{max} values, the greater the competitive effect of silicate on the adsorption to goethite. The changes in the K_{ads} and θ_{max} values reflect the combination of changes in the aqueous speciation of phosphate and silicate and changes in the structure and charging of the mineral−water interface. The results in Figure 3 further confirm that in order to have a significant competitive effect of dissolved silicate on phosphate adsorption to goethite both relatively high dissolved silicate concentrations (>100 μM) and favorable pH conditions (>7) are required.

3.3. Effect of Background Electrolyte Concentration. The solution ionic strength affects the formation of both inner- and outer-sphere surface complexes, although the sensitivity to ionic strength is highest for outer-sphere complexes.[37,58,59] The type of background electrolyte also plays an important role in surface complexation reactions: the electrolyte ions may compete with the sorbate for surface binding sites, form strong aqueous complexes with the sorbate, and change the charge distribution and thickness of the electrical double layer.[37,54,58,59]

The CD-MUSIC model simulations predict a relatively small effect of increasing the NaCl concentration from 10 mM to 1 M on phosphate adsorption to goethite (Figure 4a). At pH 7 for instance the amount of adsorbed phosphate in the presence of 10 mM NaCl is 1.77 μmol/m^2, compared to 1.91 μmol/m^2 at 0.5 M NaCl. The effect likely reflects a more positive surface charge due to Na$^+$ adsorption, creating a more favorable electrostatic environment for aqueous phosphate binding to the goethite surface. However, when doubling the NaCl concentration from 0.5 to 1 M, the adsorption of phosphate to goethite drops slightly by 0.7%, potentially because of competitive adsorption by chloride anions. The model further predicts a weakening of the NaCl enhanced adsorption of phosphate below pH 5.5.

Variations in ionic strength also have a limited influence on silicate adsorption above pH 9. The pH-dependent trend, however, is quite different from that of phosphate (Figure 4c). As for phosphate, increasing the NaCl concentration (from 10 mM to 1 M) decreases silicate sorption but this effect of NaCl becomes negligible above pH 9, consistent with the formation of inner-sphere complexes. Below pH 9, silicate adsorption may be enhanced due to the neutralization of negative surface charge by Na$^+$ adsorption.[37] When silicate is present, the combined NaCl effects cause a reversal around pH 8 in the response of phosphate adsorption to increasing NaCl concentration (Figure 4b). Nonetheless, the predicted weak response of phosphate adsorption to the 2 orders of magnitude change in the NaCl concentration implies the formation of strong inner-sphere phosphate surface complexes.

3.4. Desorption of Phosphate. In the desorption experiment, goethite was first equilibrated with phosphate at pH 3, which led to the uptake of 61% of the initial aqueous phosphate (25 μM). As expected, the stepwise pH increase from 3 to 11 resulted in a gradual release of the adsorbed phosphate. In Figure 5, The amount of desorbed phosphate at a given pH is compared to that calculated by the CD-MUSIC model assuming that the mineral-water interface remains in thermodynamic equilibrium with the aqueous solution. As can be seen, less phosphate desorbed than predicted by the model, with the difference increasing along the transition from acidic to alkaline conditions. For example, 21% of the initially
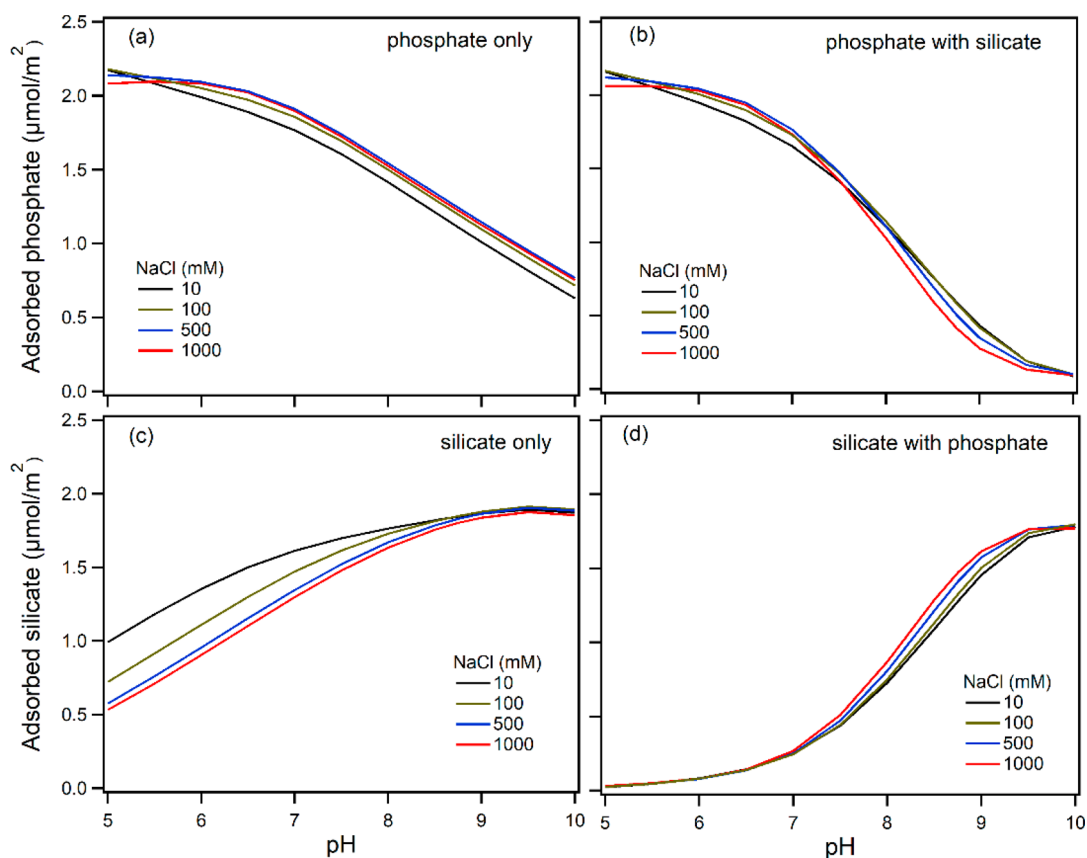
Figure 4. (top) Adsorption of phosphate (25 μM) in the (a) absence and (b) presence of silicate (250 μM) on goethite (0.5 g/L) at 25 °C with varying NaCl concentrations (10−1000 mM). (bottom) Silicate adsorption data in the (c) absence and (d) presence of phosphate under the experimental conditions stated above. The adsorption data are calculated using the CD-MUSIC model with the parameters presented in Table 1.
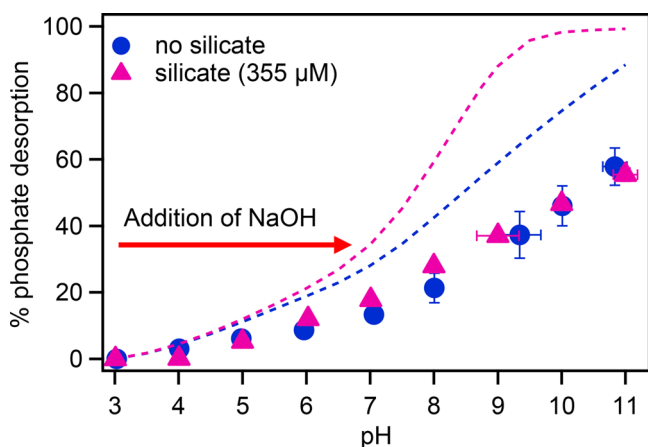
Figure 5. Percentage of phosphate desorption from goethite as a function of pH, in the absence (filled circles) and presence of 355 μM silicate (filled triangles), with respect to the amount sorbed at pH 3. The phosphate (25 μM) solution prepared in 10 mM NaCl was equilibrated with goethite (0.5 g/L) at pH 3 and at 22 °C, which resulted in about 62% adsorption (~2.11 μmol/m^2) of the initial aqueous phosphate. The dashed lines represent the CD-MUSIC model prediction in the absence (blue) and presence of silicate (pink). Error bars represent the range of values measured between duplicate experiments.

adsorbed phosphate is recovered in solution at pH 7. In the absence of silicate, however, the model predicts 42% desorption, a 21% difference. This difference increases to 30% at pH 8. With further increase in pH, the difference

between experimental results and model predictions stays fairly constant (Figure 5), at about 0.5 μmol/m^2. The latter is comparable to the amount removed from solution during the slow uptake phase in the kinetic phosphate sorption experiments at pH 7 (see Supporting Information Table S1).

The results in Figure 5 indicate that a fraction of the phosphate initially sorbed at pH 3 remains irreversibly bound to goethite, at the time scale of the desorption experiment (>70 h). Several mechanisms may explain this. For example, phosphate in long-term contact with goethite may form strong bridging complexes with iron dissolved from the solid phase,[60] limiting phosphate release back into solution. The transformation of relatively weak outer-sphere and monodentate phosphate−goethite surface complexes to the more stable bidentate complexes has also been suggested to take place with increasing solution pH.[61] The detachment of bidentate phosphate complexes is thermodynamically and kinetically less favorable compared to their formation on ferric iron (hydr)oxide surfaces.[62] The first, presumably rate-limiting, step in the desorption of a bidentate complex requires the cleavage of a strong O_3PO-Fe bond producing a monodentate complex.[62] A gradual diffusion of adsorbed phosphate into the lattice structure of the mineral is also possible, further augmenting the irreversibly bound phosphate pool.[63,64]

The presence of silicate has no measurable effect on the desorption of adsorbed phosphate from goethite during the pH increase from 3 to 11 (Figure 5), despite an initial dissolved silicate concentration ~15 times higher than that of phosphate. That is, the expected enhanced desorption of phosphate due to

the competitive adsorption of silicate under alkaline conditions is not observed. Most likely, once phosphate is strongly bound to the goethite surface lattice it can no longer be displaced by silicate. The inability of even high concentrations of dissolved silicate to mobilize phosphate bound to natural sediment particles has also been reported by Tuominen et al.[28] Thus, while during phosphate adsorption the effect of silicate can be explained by equilibrium surface reactions, kinetic factors prevent silicate from having a measurable effect on phosphate desorption.

4. CONCLUSIONS

In this study, we investigated the competitive effects of aqueous silicate on phosphate adsorption onto and desorption from goethite over a broad range of pH. The adsorption data are successfully reproduced by the CD-MUSIC model. Model simulations predict that dissolved silicate can significantly decrease phosphate adsorption on goethite above pH 7 and at high aqueous Si:P molar ratios, such as can be found in alkaline lakes in volcanic areas. The competitive effect of silicate is minor below neutral pH even in the presence of high concentrations of dissolved silicate. Results from the phosphate desorption experiment show that a transition from acidic to alkaline conditions results in the incomplete desorption of phosphate, pointing to a fraction of adsorbed phosphate that has become irreversibly bound to the mineral. Even under alkaline conditions, dissolved silicate is unable to displace these strongly bound phosphate ions. The release to solution of this fraction of mineral-bound phosphate, and therefore, its return to the bioavailable P pool, can probably only be achieved through the reductive dissolution of the goethite. It should be noted that the phosphate and silicate adsorption experiments were conducted in the simple NaCl background electrolyte solutions in this study. However, the chemical compositions of natural waters are more complex and contain other major anions (e.g., HCO_3^- and SO_4^{2-}) and cations (e.g., Ca^{2+} and Mg^{2+}). In addition, temperature is also an additional environmental factor that can modulate the competitive interactions between phosphate and silicate at the goethite−water interface. Therefore, further studies should give continued attention to the role of variable aqueous composition in modulating the exchanges of phosphate between solution and the surfaces of ferric iron (hydr)oxides, as well as to the effect of temperature and the relative importance of adsorption versus additional processes controlling the mineral−water partitioning of phosphate, in particular the oxidative precipitation and reductive dissolution of ferric iron (hydr)oxides.

■ ASSOCIATED CONTENT

Ⓢ Supporting Information

The Supporting Information is available free of charge at https://pubs.acs.org/doi/10.1021/acsearthspace-chem.1c00197.

> Phosphate adsorption kinetics, calculation of root-mean-square error (RMSE) and chi-squared values, phosphate desorption kinetics, phosphate and silicate adsorption (data and CD-MUSIC modeling), assessment of the CD-MUSIC model, major anions in surface waters (US National Water Information System (NWIS) data) (PDF)

■ AUTHOR INFORMATION

Corresponding Author

Md Abdus Sabur − *Ecohydrology Research Group, Department of Earth and Environmental Sciences, University of Waterloo, Waterloo, ON N2L 3G1, Canada; Water Institute, University of Waterloo, Waterloo, ON N2L 3G1, Canada; Department of Chemistry, Jahangirnagar University, Savar, Dhaka 1342, Bangladesh;* ⓞ orcid.org/0000-0002-9800-8937; Email: sabur@juniv.edu

Authors

Christopher T. Parsons − *Ecohydrology Research Group, Department of Earth and Environmental Sciences, University of Waterloo, Waterloo, ON N2L 3G1, Canada; Water Institute, University of Waterloo, Waterloo, ON N2L 3G1, Canada; Watershed Hydrology and Ecology Research Division, Environment and Climate Change Canada, Burlington, ON L7S 1A1, Canada*

Taylor Maavara − *School of the Environment, and Yale Institute for Biospheric Studies, Yale University, New Haven, Connecticut 06511, United States*

Philippe Van Cappellen − *Ecohydrology Research Group, Department of Earth and Environmental Sciences, University of Waterloo, Waterloo, ON N2L 3G1, Canada; Water Institute, University of Waterloo, Waterloo, ON N2L 3G1, Canada;* ⓞ orcid.org/0000-0001-5476-0820

Complete contact information is available at:
https://pubs.acs.org/10.1021/acsearthspacechem.1c00197

Notes

The authors declare no competing financial interest.

■ ACKNOWLEDGMENTS

■ REFERENCES

(1) Schindler, D. W. Evolution of Phosphorus Limitation in Lakes. *Science (Washington, DC, U. S.)* **1977**, *195* (4275), 260−262.

(2) Smith, V. H.; Schindler, D. W. Eutrophication Science: Where Do We Go from Here? *Trends Ecol. Evol.* **2009**, *24* (4), 201−207.

(3) Carpenter, S. R. Phosphorus Control Is Critical to Mitigating Eutrophication. *Proc. Natl. Acad. Sci. U. S. A.* **2008**, *105* (32), 11039−11040.

(4) Correll, D. L. The Role of Phosphorus in the Eutrophication of Receiving Waters: A Review. *J. Environ. Qual.* **1998**, *27* (2), 261.

(5) Scavia, D.; David Allan, J.; Arend, K. K.; Bartell, S.; Beletsky, D.; Bosch, N. S.; Brandt, S. B.; Briland, R. D.; Daloğlu, I.; DePinto, J. V.; Dolan, D. M.; Evans, M. A.; Farmer, T. M.; Goto, D.; Han, H.; Höök, T. O.; Knight, R.; Ludsin, S. A.; Mason, D.; Michalak, A. M.; Peter Richards, R.; Roberts, J. J.; Rucinski, D. K.; Rutherford, E.; Schwab, D. J.; Sesterhenn, T. M.; Zhang, H.; Zhou, Y. Assessing and Addressing the Re-Eutrophication of Lake Erie: Central Basin Hypoxia. *J. Great Lakes Res.* **2014**, *40* (2), 226−246.

(6) Orihel, D. M.; Baulch, H. M.; Casson, N. J.; North, R. L.; Parsons, C. T.; Seckar, D. C. M.; Venkiteswaran, J. J. Internal Phosphorus Loading in Canadian Fresh Waters: A Critical Review and Data Analysis. *Can. J. Fish. Aquat. Sci.* **2017**, *74* (12), 2005−2029.

(7) Matisoff, G.; Kaltenberg, E. M.; Steely, R. L.; Hummel, S. K.; Seo, J.; Gibbons, K. J.; Bridgeman, T. B.; Seo, Y.; Behbahani, M.; James, W. F.; Johnson, L. T.; Doan, P.; Dittrich, M.; Anne, M.; Chaf, J. D.; et al. Internal Loading of Phosphorus in Western Lake Erie. *J. Great Lakes Res.* **2016**, *42* (4), 775−788.

(8) Matisoff, G.; Watson, S. B.; Guo, J.; Duewiger, A.; Steely, R. Sediment and Nutrient Distribution and Resuspension in Lake Winnipeg. *Sci. Total Environ.* **2017**, *575*, 173−186.

(9) Paytan, A.; Roberts, K.; Watson, S.; Peek, S.; Chuang, P.; Defforey, D.; Kendall, C. Internal Loading of Phosphate in Lake Erie Central Basin. *Sci. Total Environ.* **2017**, *579*, 1356−1365.

(10) Nürnberg, G. K.; Lazerte, B. D. More than 20 Years of Estimated Internal Phosphorus Loading in Polymictic, Eutrophic Lake Winnipeg. *J. Great Lakes Res.* **2016**, *42* (1), 18−27.

(11) Kim, D.; Peller, T.; Gozum, Z.; Theÿsmeÿer, T.; Long, T.; Boyd, D.; Watson, S.; Rao, Y. R.; Arhonditsis, G. B. Modelling Phosphorus Dynamics in Cootes Paradise Marsh: Uncertainty Assessment and Implications for Eutrophication Management. *Aquat. Ecosyst. Health Manage.* **2016**, *19* (4), 368−381.

(12) O'Connell, D. W.; Ansems, N.; Kukkadapu, R. K.; Jaisi, D.; Orihel, D. M.; Cade-Menun, B. J.; Van Cappellen, P.; et al. Changes in Sedimentary Phosphorus Burial Following Artificial Eutrophication of Lake 227, Experimental Lakes Area, Ontario, Canada. *J. Geophys. Res.: Biogeosci.* **2020**, *125* (8), e2020JG005713.

(13) Audette, Y.; Smith, D. S.; Parsons, C. T.; Chen, W.; Rezanezhad, F.; Van Cappellen, P. Phosphorus Binding to Soil Organic Matter via Ternary Complexes with Calcium. *Chemosphere* **2020**, *260*, 127624.

(14) Christophoridis, C.; Fytianos, K. Conditions Affecting the Release of Phosphorus from Surface Lake Sediments. *J. Environ. Qual.* **2006**, *35* (4), 1181−1192.

(15) Zhu, Y.; Wu, F.; He, Z.; Guo, J.; Qu, X.; Xie, F.; et al. Characterization of Organic Phosphorus in Lake Sediments by Sequential Fractionation and Enzymatic Hydrolysis. *Environ. Sci. Technol.* **2013**, *47* (14), 7679−7687.

(16) Oxmann, J. F.; Schwendenmann, L. Authigenic Apatite and Octacalcium Phosphate Formation Due to Adsorption − Precipitation Switching across Estuarine Salinity. *Biogeosciences* **2015**, *12*, 723−738.

(17) Smolders, A. J. P.; Lamers, L. P. M.; Lucassen, E. C. H. E. T.; Van Der Velde, G.; Roelofs, J. G. M. Internal Eutrophication: How It Works and What to Do about It − a Review. *Chem. Ecol.* **2006**, *22* (2), 93−111.

(18) Joshi, S. R.; Kukkadapu, R. K.; Burdige, D. J.; Bowden, M. E.; Sparks, D. L.; Jaisi, D. P. Organic Matter Remineralization Predominates Phosphorus Cycling in the Mid-Bay Sediments in the Chesapeake Bay. *Environ. Sci. Technol.* **2015**, *49* (10), 5887−5896.

(19) Antelo, J.; Arce, F.; Avena, M.; Fiol, S.; López, R.; Macías, F. Adsorption of a Soil Humic Acid at the Surface of Goethite and Its Competitive Interaction with Phosphate. *Geoderma* **2007**, *138* (1−2), 12−19.

(20) Geelhoed, J. S.; Hiemstra, T.; Van Riemsdijk, W. H. Phosphate and Sulfate Adsorption on Goethite: Single Anion and Competitive Adsorption. *Geochim. Cosmochim. Acta* **1997**, *61* (12), 2389−2396.

(21) Iler, R. K. *The Chemistry of Silica: Solubility, Polymerization, Colloid and Surface Properties, and Biochemistry*; Wiley and Sons: Chichester, 1979.

(22) Struyf, E.; Smis, A.; Van Damme, S.; Meire, P.; Conley, D. J. The Global Biogeochemical Silicon Cycle. *Silicon* **2009**, *1* (4), 207−213.

(23) Sabur, M. A. *Interactions of Phosphate and Silicate with Iron Oxides in Freshwater Environments*; University of Waterloo, 2019.

(24) Loucaides, S.; Van Cappellen, P.; Roubeix, V.; Moriceau, B.; Ragueneau, O. Controls on the Recycling and Preservation of Biogenic Silica from Biomineralization to Burial. *Silicon* **2012**, *4* (1), 7−22.

(25) Koszelnik, P.; Tomaszek, J. a. Dissolved Silica Retention and Its Impact on Eutrophication in a Complex of Mountain Reservoirs. *Water, Air, Soil Pollut.* **2008**, *189* (1−4), 189−198.

(26) Koski-Vähälä, J.; Hartikainen, H.; Tallberg, P. Phosphorus Mobilization from Various Sediment Pools in Response to Increased PH and Silicate Concentration. *J. Environ. Qual.* **2001**, *30* (2), 546−552.

(27) Tallberg, P.; Tréguer, P.; Beucher, C.; Corvaisier, R. Potentially Mobile Pools of Phosphorus and Silicon in Sediment from the Bay of Brest: Interactions and Implications for Phosphorus Dynamics. *Estuarine, Coastal Shelf Sci.* **2008**, *76* (1), 85−94.

(28) Tuominen, L.; Hartikainen, H.; Kairesalo, T.; Tallberg, P. Increases Bioavaliability of Sediment Phosphorus Due to Silicate Enrichment. *Water Res.* **1998**, *32* (7), 2001−2008.

(29) Schaller, J.; Faucherre, S.; Joss, H.; Obst, M.; Goeckede, M.; Planer-Friedrich, B.; Peiffer, S.; Gilfedder, B.; Elberling, B. Silicon Increases the Phosphorus Availability of Arctic Soils. *Sci. Rep.* **2019**, *9* (1), 1−11.

(30) Turner, B. L.; Cade-Menun, B. J.; Condron, L. M.; Newman, S. Extraction of Soil Organic Phosphorus. *Talanta* **2005**, *66* (2), 294−306.

(31) Baines, S. B.; Twining, B. S.; Vogt, S.; Balch, W. M.; Fisher, N. S.; Nelson, D. M. Elemental Composition of Equatorial Pacific Diatoms Exposed to Additions of Silicic Acid and Iron. *Deep Sea Res., Part II* **2011**, *58* (3−4), 512−523.

(32) Sabur, M. A.; Al-Abadleh, H. A. Surface Interactions of Monomethylarsonic Acid with Hematite Nanoparticles Studied Using ATR-FTIR: Adsorption and Desorption Kinetics. *Can. J. Chem.* **2015**, *93* (11), 1297−1304.

(33) Stachowicz, M.; Hiemstra, T.; van Riemsdijk, W. H. Multi-Competitive Interaction of As(III) and As(V) Oxyanions with Ca^{2+}, Mg^{2+}, PO_4^{3-}, and CO_3^{2-} Ions on Goethite. *J. Colloid Interface Sci.* **2008**, *320* (2), 400−414.

(34) Hiemstra, T.; Barnett, M. O.; van Riemsdijk, W. H. Interaction of Silicic Acid with Goethite. *J. Colloid Interface Sci.* **2007**, *310* (1), 8−17.

(35) Jordan, N.; Marmier, N.; Lomenech, C.; Giffaut, E.; Ehrhardt, J. J. Sorption of Silicates on Goethite, Hematite, and Magnetite: Experiments and Modelling. *J. Colloid Interface Sci.* **2007**, *312* (2), 224−229.

(36) Jordan, N.; Marmier, N.; Lomenech, C.; Giffaut, E.; Ehrhardt, J. J. Competition between Selenium (IV) and Silicic Acid on the Hematite Surface. *Chemosphere* **2009**, *75* (1), 129−134.

(37) Hiemstra, T. Ferrihydrite Interaction with Silicate and Competing Oxyanions: Geometry and Hydrogen Bonding of Surface Species. *Geochim. Cosmochim. Acta* **2018**, *238*, 453−476.

(38) Liu, H.; Chen, T.; Frost, R. L. An Overview of the Role of Goethite Surfaces in the Environment. *Chemosphere* **2014**, *103*, 1−11.

(39) Rahnemaie, R.; Hiemstra, T.; Van Riemsdijk, W. H. Geometry, Charge Distribution, and Surface Speciation of Phosphate on Goethite. *Langmuir* **2007**, *23* (7), 3680−3689.

(40) Vakros, J.; Kordulis, C.; Lycourghiotis, A. Potentiometric Mass Titrations: A Quick Scan for Determining the Point of Zero Charge. *Chem. Commun.* **2002**, 1980−1981.

(41) Kanematsu, M.; Young, T. M.; Fukushi, K.; Sverjensky, D. A.; Green, P. G.; Darby, J. L. Quantification of the Effects of Organic and Carbonate Buffers on Arsenate and Phosphate Adsorption on a Goethite-Based Granular Porous Adsorbent. *Environ. Sci. Technol.* **2011**, *45* (2), 561−568.

(42) Hartikainen, H.; Pitkänen, M.; Kairesalo, T.; Tuominen, L. Co-Occurrence and Potential Chemical Competition of Phosphorus and Silicon in Lake Sediment. *Water Res.* **1996**, *30* (10), 2472−2478.

(43) Hiemstra, T.; De Wit, J. C. M.; Van Riemsdijk, W. H. Multisite Proton Adsorption Modeling at the Solid/Solution Interface of (Hydr)Oxides: A New Approach: II. Application to Various Important (Hydr)Oxides. *J. Colloid Interface Sci.* **1989**, *133* (1), 105−117.

(44) Hiemstra, T.; Van Riemsdijk, W. H.; Bolt, G. H. Multisite Proton Adsorption Modeling at the Solid/Solution Interface of (Hydr) Oxides: A New Approach: I. Model Description and Evaluation of Intrinsic Reaction Constants. *J. Colloid Interface Sci.* **1989**, *133* (1), 91−104.

(45) Hiemstra, T.; van Riemsdijk, W. H. A Surface Structural Approach to Ion Adsorption: The Charge Distribution (CD) Model. *J. Colloid Interface Sci.* **1996**, *179* (2), 488−508.

(46) Hiemstra, T.; Van Riemsdijk, W. H. Surface Structural Ion Adsorption Modeling of Competitive Binding of Oxyanions by Metal (Hydr)Oxides. *J. Colloid Interface Sci.* **1999**, *210* (1), 182−193.

(47) Hiemstra, T.; Van Riemsdijk, W. H. On the Relationship between Charge Distribution, Surface Hydration, and the Structure of the Interface of Metal Hydroxides. *J. Colloid Interface Sci.* **2006**, *301*, 1−18.

(48) Antelo, J.; Fiol, S.; Pérez, C.; Mariño, S.; Arce, F.; Gondar, D.; López, R. Analysis of Phosphate Adsorption onto Ferrihydrite Using the CD-MUSIC Model. *J. Colloid Interface Sci.* **2010**, *347* (1), 112−119.

(49) Brown, D.; Altermatt, D. Bond-Valence Parameters Obtained from a Systematic Analysis of the Inorganic Crystal Structure Satabase. *Acta Crystallogr., Sect. B: Struct. Sci.* **1985**, *B41* (4), 244−247.

(50) Kersten, M.; Vlasova, N. Silicate Adsorption by Goethite at Elevated Temperatures. *Chem. Geol.* **2009**, *262* (3−4), 336.

(51) Rahnemaie, R.; Hiemstra, T.; van Riemsdijk, W. H. Carbonate Adsorption on Goethite in Competition with Phosphate. *J. Colloid Interface Sci.* **2007**, *315* (2), 415−425.

(52) Parkhurst, D. L.; Appelo, C. A. J. *Description of Input and Examples for PHREEQC Version 3--a Computer Program for Speciation, Batch-Reaction, One-Dimensional Transport, and Inverse Geochemical Calculations: U.S. Geological Survey Techniques and Methods*; U.S. Geological Survey, 2013.

(53) Kinniburgh, D. G.; Copper, D. M. Surface Complexation (CD-MUSIC): Cdmusic_hiemstra.Dat. 2011; phreeplot.org/ppihtml/cdmusic_hiemstra.dat.html.

(54) Spiteri, C.; Cappellen, P. V.; Regnier, P. Surface Complexation Effects on Phosphate Adsorption to Ferric Iron Oxyhydroxides along PH and Salinity Gradients in Estuaries and Coastal Aquifers. *Geochim. Cosmochim. Acta* **2008**, *72*, 3431−3445.

(55) Gao, Y.; Mucci, A. Acid Base Reactions, Phosphate and Arsenate Complexation, and Their Competitive Adsorption at the Surface of Goethite in 0.7 M NaCl Solution. *Geochim. Cosmochim. Acta* **2001**, *65* (14), 2361−2378.

(56) Swedlund, P. J.; Webster, J. G. Adsorption and Polymerisation of Silicic Acid on Ferrihydrite, and Its Effect on Arsenic Adsorption. *Water Res.* **1999**, *33* (16), 3413−3422.

(57) Langmuir, D. *Aqueous Environmental Geochemistry*; McConnin, R., Ed.; Prentice-Hall. Inc.: NJ, 1997.

(58) Antelo, J.; Avena, M.; Fiol, S.; López, R.; Arce, F. Effects of PH and Ionic Strength on the Adsorption of Phosphate and Arsenate at the Goethite-Water Interface. *J. Colloid Interface Sci.* **2005**, *285* (2), 476−486.

(59) Goldberg, S. Application of Surface Complexation Models to Anion Adsorption by Natural Materials. *Environ. Toxicol. Chem.* **2014**, *33* (10), 2172−2180.

(60) Ler, A.; Stanforth, R. Evidence for Surface Precipitation of Phosphate on Goethite. *Environ. Sci. Technol.* **2003**, *37* (12), 2694−2700.

(61) Zhong, B.; Stanforth, R.; Wu, S.; Chen, J. P. Proton Interaction in Phosphate Adsorption onto Goethite. *J. Colloid Interface Sci.* **2007**, *308*, 40−48.

(62) Farrell, J.; Chaudhary, B. K. Understanding Arsenate Reaction Kinetics with Ferric Hydroxides. *Environ. Sci. Technol.* **2013**, *47* (15), 8342−8347.

(63) Fuller, C. C.; Davis, J. A. M. A.; Waychunas, G. A. Surface Chemistry of Ferrihydrite: Part 2. Kinetics of Arsenate Adsorption and Coprecipitation. *Geochim. Cosmochim. Acta* **1993**, *57* (10), 2271−2282.

(64) Luengo, C.; Brigante, M.; Avena, M. Adsorption Kinetics of Phosphate and Arsenate on Goethite. A Comparative Study. *J. Colloid Interface Sci.* **2007**, *311* (2), 354−360.